

Functional and Spatial Regulation of Mitotic Centromere-Associated Kinesin by Cyclin-Dependent Kinase 1^{∇†}

Mourad Sanhaji,¹ Claire Therese Friel,² Nina-Naomi Kreis,¹ Andrea Krämer,¹ Claudia Martin,² Jonathon Howard,² Klaus Strebhardt,^{1‡} and Juping Yuan^{1‡*}

Department of Gynecology and Obstetrics, School of Medicine, J. W. Goethe University, Theodor-Stern-Kai 7, D-60590 Frankfurt, Germany,¹ and MPI-CBG, Pfotenhauerstr. 108, D-01307 Dresden, Germany²

Received 27 January 2010/Returned for modification 10 February 2010/Accepted 24 March 2010

Mitotic centromere-associated kinesin (MCAK) plays an essential role in spindle formation and in correction of improper microtubule-kinetochore attachments. The localization and activity of MCAK at the centromere/kinetochore are controlled by Aurora B kinase. However, MCAK is also abundant in the cytosol and at centrosomes during mitosis, and its regulatory mechanism at these sites is unknown. We show here that cyclin-dependent kinase 1 (Cdk1) phosphorylates T537 in the core domain of MCAK and attenuates its microtubule-destabilizing activity *in vitro* and *in vivo*. Phosphorylation of MCAK by Cdk1 promotes the release of MCAK from centrosomes and is required for proper spindle formation. Interfering with the regulation of MCAK by Cdk1 causes dramatic defects in spindle formation and in chromosome positioning. This is the first study demonstrating that Cdk1 regulates the localization and activity of MCAK in mitosis by directly phosphorylating the catalytic core domain of MCAK.

Chromosomes are properly attached to the mitotic spindles, and chromosome movement is tightly linked to the structure and dynamics of spindle microtubules during mitosis. Important regulators of microtubule dynamics are the kinesin-13 proteins (37). This kinesin superfamily is defined by the localization of the conserved kinesin core motor domain in the middle of the polypeptide (19). Kinesin-13 proteins induce microtubule depolymerization by disassembling tubulin subunits from the polymer end (6). Among them, mitotic centromere-associated kinesin (MCAK) is the best-characterized member of the family. It depolymerizes microtubules *in vitro* and *in vivo*, regulates microtubule dynamics, and has been implicated in correcting misaligned chromosomes (12, 14, 16, 24). In agreement with these observations, both overexpression and inhibition of MCAK result in a disruption of microtubule dynamics, leading further to improper spindle assembly and errors in chromosome alignment and segregation (7, 11, 15, 22, 33). The importance of MCAK in ensuring the faithful segregation of chromosomes is consistent with the observation that MCAK is highly expressed in several types of cancer and thus is likely to be involved in causing aneuploidy (25, 32).

While MCAK is found both in the cytoplasm and at the centromeres throughout the cell cycle, it is highly enriched on centrosomes, the centromeres/kinetochores, and the spindle midzone during mitosis (18, 21, 36, 38). In accordance with its localizations, MCAK affects many aspects throughout mitosis, from spindle assembly and maintenance (3, 10, 36) to chromosome positioning and segregation (14, 21, 35). Thus, the pre-

cise control of the localization and activity of MCAK is crucial for maintaining genetic integrity during mitosis. Regulation of MCAK on the centromeres/kinetochores by Aurora B kinase in mitosis has been intensively investigated (1, 28, 29, 43). The data reveal that MCAK is phosphorylated on several serine/threonine residues by Aurora B, which inhibits the microtubule-destabilizing activity of MCAK and regulates its localization on chromosome arms/centromeres/kinetochores during mitosis (1, 18, 28). Moreover, in concert with Aurora B, ICIS (inner centromere KinI stimulator), a protein targeting the inner centromeres in an MCAK-dependent manner, may regulate MCAK at the inner centromeres and prevent kinetochore-microtubule attachment errors in mitosis by stimulating the activity of MCAK (27). Interestingly, hSgo2, a recently discovered inner centromere protein essential for centromere cohesion, has been reported to be important in localizing MCAK to the centromere and in spatially regulating its mitotic activity (13). These data highlight that the activity and localization of MCAK on the centromeres/kinetochores during mitosis are tightly controlled by Aurora B and its cofactors. Remarkably, MCAK concentrates at spindle poles from prophase to telophase during mitosis (18); however, only a few studies have been done to deal with that issue. Aurora A-depleted prometaphase cells delocalize MCAK from spindle poles but accumulate the microtubule-stabilizing protein ch-TOG at poles (5), implying that Aurora A might influence the centrosomal localization of MCAK in mitosis. Aurora A is also found to be important for focusing microtubules at aster centers and for facilitating the transition from asters to bipolar spindles in *Xenopus* egg extracts (42). In addition, it has been revealed that Ca²⁺/calmodulin-dependent protein kinase II gamma (CaMKII gamma) suppresses MCAK's activity, which is essential for bipolar spindle formation in mitosis (11). More work is required to gain insight into the regulatory mechanisms of MCAK at spindle poles during mitosis.

Deregulated cyclin-dependent kinases (Cdks) are very often

* Corresponding author. Mailing address: Department of Gynecology and Obstetrics, School of Medicine, J. W. Goethe University, Theodor-Stern-Kai 7, 60590 Frankfurt, Germany. Phone: 49 69 6301 5819. Fax: 49 69 6301 6364. E-mail: yuan@em.uni-frankfurt.de.

† Supplemental material for this article may be found at <http://mcb.asm.org/>.

‡ Both contributed equally as last authors.

∇ Published ahead of print on 5 April 2010.

linked to genomic and chromosomal instability (20). Cyclin B1, the regulatory subunit of Cdk1, is localized to unattached kinetochores and contributes to efficient microtubule attachment and proper chromosome alignment (2, 4). We observed that knockdown of cyclin B1 induces defects in chromosome alignment and mitotic spindle formation (N.-N. Kreis, M. Sanhaji, A. Krämer, K. Sommor, F. Rödel, K. Strebhardt, and J. Yuan, submitted for publication). Yet, how Cdk1/cyclin B1 carries out these functions is not very well understood. In this context, it is extremely interesting to investigate the relationship between the essential mitotic kinase Cdk1 and the microtubule depolymerase MCAK in human cells.

MATERIALS AND METHODS

Cell culture, synchronization, and preparation of cellular extracts. HeLa, SW-480, MCF-7, and Saos-2 cells were grown according to the supplier's suggestions (DSMZ, Braunschweig, Germany). Cells were synchronized to the G₁/S boundary with a double thymidine block and to prometaphase with thymidine/nocodazole treatment (17). Cell lysis was performed with radioimmunoprecipitation assay (RIPA) buffer (17). HeLa 776-6 cells were established as described previously (40). Briefly, HeLa cells transfected with plasmids pH1/shRNA/cyclin B1 were selected with medium containing G418 for 6 weeks. Cell clones with various cyclin B1 levels were obtained.

Western blot analysis and MCAK phospho-specific-antibody generation. Western blot analysis was performed as described previously (17), using the following antibodies: mouse monoclonal anti-KIF2C (Abnova, Taipei, Taiwan), mouse monoclonal anti-cyclin B1 (Santa Cruz Biotechnology, Heidelberg, Germany), rabbit polyclonal anti-cyclin B1 (Santa Cruz Biotechnology), mouse monoclonal anti-Cdk1 (Santa Cruz Biotechnology), mouse monoclonal anti-glutathione S-transferase (anti-GST) (Santa Cruz Biotechnology), rabbit polyclonal anti-phospho-Cdk1Thr161 (Cell Signaling, Boston, MA), mouse monoclonal anti-FLAG M2 (Sigma-Aldrich, Taufkirchen, Germany), and mouse monoclonal anti- β -actin (Sigma-Aldrich). To generate polyclonal antibodies against MCAK phosphorylated on T537, rabbits were immunized using the peptide CGQNKAHpTPFPRES (pT is phospho-T), and antibodies were affinity purified (Eurogentec, Seraing, Belgium).

siRNA and transfection. Two small interfering RNAs (siRNAs) targeting human MCAK (NCBI accession number NM 006845) were synthesized by Sigma-Aldrich, referred to as siRNA MCAK1 against positions 1666 to 1686 of the coding frame and siRNA MCAK2 against positions 11 to 31 of the 3' untranslated region. Control siRNA was purchased from Dharmacon Research, Inc. (Lafayette, CO). All siRNAs were 21 nucleotides in length and contained symmetric 3' overhangs of two deoxythymidines. Cells were transfected with siRNA using the transfection reagent Oligofectamine as described previously (41). Transient transfections were carried out using FuGENE-6 transfection reagent, as instructed (Roche Applied Science, Mannheim, Germany). For phenotype analysis, HeLa cells depleted of endogenous MCAK were cotransfected with Flag-tagged MCAK and pBabe-puro constructs (a kind gift from X. Q. Liu, Purdue University) at a ratio of 10:1. After selection with 2 μ g/ml puromycin, floating cells were washed away and attached cells were cultured for further phenotypic analyses, including cell cycle analysis, quantification of polymerized tubulin in cells, intercentromere distance measurement, and indirect immunofluorescence for assessment of chromosome positioning and abnormal spindle formation. All experiments were independently performed at least three times.

Construction of DNA plasmids and recombinant protein expression. Full-length human MCAK cDNA pCMV-SPORT6-Kif2c was obtained from RZPD (clone IRATp970F0111D; Berlin, Germany). By use of primers 5'-ATGGCCA TGGACTCGTTCAGG-3' and 5'-TCACTGGGGCCGTTTCTTGCTGCTC TTAT-3', the cDNA was amplified by PCR and subcloned into the BamHI/EcoRI sites of pGEX-5x3 (GE Healthcare, Munich, Germany), into the EcoRI/BamHI sites of 3xFlag-CMV 7.1 (Invitrogen) or into the XhoI/EcoRI sites of EGFP-C2 (Invitrogen). Various domains of MCAK were also amplified and subcloned into the pGEX-5x3 plasmid by use of the following primers: for the N terminus (amino acids [aa] 1 to 187), an up primer (5'-ATGGCCATGGACTC GTCCGTTTCAGG-3') and a down primer (5'-AACTGAGTTCACAGGGTTT GCAGAAGAGCT-3'); for the neck (aa 188 to 255), an up primer (5'-CTCAG GATTCCGGTTCGAGGAAATCATGTCTGTG-3') and a down primer (5'-AACTGAGTTCACAGGGTTTGCAGAAGAGCT-3'); for the core (aa 256 to 590), an up primer (5'-AGGAAACGCCCACTGAATAAGCAAG-3') and a

down primer (5'-ACTGTGGGGGCTCAGTCCTTGACCCTGTC-3'); and for the C terminus (aa 591 to 725), an up primer (5'-GGGCCCCAGTGAGAGC AGTTGATT-3') and a down primer (5'-TCACTGGGGCCGTTTCTTGCTGCTC TTAT-3'). Point mutations were generated with a QuikChange site-directed mutagenesis kit (Stratagene, Amsterdam, Netherlands) using the following primers: for T537A, an up primer (5'-AGAACAAGGCTCAGCCCCGTTCCGTG AG-3') and a down primer (5'-CTCACGGAACGGGGCGTGAGCCTTGTTT T-3'); for T537E, an up primer (5'-GGACAGAACAAGGCTCAGCAACCGT TCCGTGAGAGCAAG-3') and a down primer (5'-CTTGCTCTCACGGAAC GGTTCTGAGCCTTGTCTGTCC-3'); and for S566A, an up primer (5'-C ATGATTGCCACGATCGCACCAGGCATAAGTC-3') and a down primer (5'-GAGCTTATGCTGGTTCGATCGTGGCAATCATG-3'). All mutant constructs were confirmed by DNA sequencing. Recombinant full-length MCAK and domains of MCAK were induced and expressed in *Escherichia coli* BL21(DE3)CodonPlus cells at 37°C for 2 h by addition of 1 mM IPTG (isopropyl- β -D-thiogalactopyranoside) and purified using glutathione-Sepharose 4B beads (GE Healthcare) as described previously (39).

Kinase assay *in vitro*. GST-tagged MCAK and subdomain proteins were incubated with Cdk1/cyclin B1 kinase (New England Biolabs, Frankfurt, Germany) in the presence of 2 μ Ci [γ -³²P]ATP and 100 μ M nonradioactive ATP at 30°C for 30 min. The reaction was stopped by adding sample buffer and boiling for 5 min. Equal volumes of each reaction were loaded onto 10% SDS-PAGE gel and separated. The gel was stained with Coomassie blue and scanned as an input control. The incorporation of ³²P was quantified using a Kodak Geldoc system.

Quantification of microtubule depolymerase activity *in vitro* and *in vivo* and ATP hydrolysis assay *in vitro*. Human MCAK-His₆ and its mutants MCAK T537E and MCAK T537A were expressed and purified as previously described (9). Briefly, depolymerization assays were carried out using GMPCPP stabilized microtubules immobilized in microscope chambers. Assays were carried out with BRB20 buffer supplemented with 75 mM KCl, 1 mM ATP, 0.1 mg/ml bovine serum albumin (BSA), 1% β -mercaptoethanol, 40 mM glucose, 40 μ g/ml glucose oxidase, and 16 μ g/ml catalase, and depolymerization was initiated by addition of a saturating concentration (500 nM) of either wild-type MCAK (MCAK WT), T537E, or T537A. The rates of depolymerization of individual microtubules in the field of view were calculated, as described previously (9). For quantification of microtubule-destabilizing activity *in vivo*, HeLa cells were depleted of endogenous MCAK by use of siRNA MCAK2 on day 1, and Flag-tagged MCAK plasmids and pBabe-puro constructs were added back on day 2. After selection with puromycin, cells were synchronized by double thymidine block on days 3 and 4. Ten hours after release on day 5, cells were collected for analysis of cellular microtubule polymer content after extraction, fixation, and staining for tubulin using fluorescence flow cytometry (Becton Dickinson, Heidelberg, Germany), as described previously (11, 31). Briefly, cellular soluble tubulin was preextracted in a saponin-containing microtubule stabilizing buffer {2 mM EGTA, 5 mM MgCl₂, 0.1 M PIPES [piperazine-N,N'-bis(2-ethanesulfonic acid)], pH 7.4, 0.2% saponin, and 25 nM Paclitaxel}. Resuspended cells in microtubule-stabilizing buffer were then fixed with an equal volume of a 4% paraformaldehyde solution at 37°C for 15 min. Cells were then washed and stained for α -tubulin with specific mouse monoclonal antibodies (Sigma-Aldrich) and fluorescein-conjugated rabbit anti-mouse antibodies (Dako, Hamburg, Germany), as described previously (11, 31). More than 95% of all cells were included in the acquisition gate, and 100,000 cells were examined. Fluorescence intensity was quantified using Cell Quest software (Becton Dickinson). Cells transfected with flag vector were assigned as having a microtubule polymer content of 100%. The experiments were independently performed five times, and each time was in triplicate.

The rate of ATP hydrolysis was determined by acid quenching samples of the reaction mixture containing 2 μ M MCAK or its variants with 2 mM MgATP in a buffer containing 20 mM PIPES, pH 6.9, and 75 mM potassium chloride buffer and then separating ADP from ATP for each sample by use of a C₁₈ column under isocratic flow with a running buffer containing 100 mM potassium phosphate, pH 6.5, 10 mM tetrabutylammonium bromide, and 10% acetonitrile. The relative proportions of ADP and ATP were quantified using the area under their respective peaks of absorbance at 260 nm. The rate of ATP hydrolysis per motor domain was determined from the rate of ADP production as a fraction of the total nucleotide.

Immunofluorescence and measurement of intercentromere distance. Cells transfected with MCAK constructs were fixed for 8 min with methanol (MeOH) containing 1% paraformaldehyde at -20°C. Cells were stained with following primary antibodies: fluorescein isothiocyanate (FITC)-conjugated monoclonal anti- α -tubulin (Sigma-Aldrich), mouse monoclonal anti- α -tubulin (Biozol, Eching, Germany), rabbit phospho-MCAK, rabbit polyclonal antibodies against pericentri- n (Abcam), mouse monoclonal anti-phospho-histone H3 (Ser10; Upstate), monoclonal anti-Cdc2, anti-Pik1, and anti-cyclin B1 (Santa Cruz Biotechnology). FITC-conjugated donkey anti-mouse, FITC-conjugated goat anti-rabbit, or Cy3-

conjugated goat anti-mouse (Jackson ImmunoResearch, West Grove) immunoglobulins were used as secondary antibodies. DNA was stained using DAPI (4',6-diamidino-2-phenylindol-dihydrochloride) (Roche, Mannheim, Germany). Slides were examined using an Axio Imager 7.1 microscope (Zeiss, Göttingen, Germany), and images were taken using an Axio Cam MRm camera (Zeiss, Göttingen, Germany). For the measurement of intercentromeric distances, cells were treated as described above and stained with Cenp-A antibodies (Cell Signaling). Images were acquired with 40X/63X Plan Neofluar objectives with an Axio Imager Z.1 (Carl Zeiss Imaging Solutions, Jena, Germany). Intercentromeric distances of metaphase cells were measured using AxioVision software. At least 10 cells transfected either with MCAK WT or with its mutants were examined, and 8 to 10 pairs of sister centromeres were taken for the measurement.

Statistical analysis. For assays *in vitro*, Student's *t* test was used to evaluate the significance of differences between MCAK WT and mutated MCAK or between control cells and plasmid-transfected/siRNA-treated cells. Differences were considered statistically significant when *P* was <0.05.

RESULTS

MCAK expression is cell cycle regulated, and MCAK interacts with Cdk1/cyclin B1. To explore whether Cdk1/cyclin B1 and MCAK cooperate to regulate mitotic events, we studied their expression throughout the cell cycle. As illustrated in Fig. S1A in the supplemental material, MCAK and cyclin B1, the regulatory subunit of Cdk1, exhibit similar expression/turnover kinetics. MCAK and Cdk1 were found to colocalize at centrosomes throughout mitosis (see Fig. S1B in the supplemental material). MCAK levels clearly correlated with cyclin B1 expression and the active form of Cdk1 (pT161) in breast cancer cell line MCF-7, colon cancer cell line SW-480, and osteosarcoma cell line Saos-2, in addition to HeLa cells (see Fig. S1C in the supplemental material). Moreover, Cdk1/cyclin B1 and MCAK were precipitated using either Flag antibodies with mitotic lysates from HeLa cells transfected with Flag-tagged MCAK (see Fig. S1D in the supplemental material) or antibodies against cyclin B1 or Cdk1 with mitotic lysates from nontransfected HeLa cells (see Fig. S1E in the supplemental material). This precipitation was not observed with interphase extracts (data not shown).

Cdk1 phosphorylates T537 in the core domain of MCAK. To analyze the role of Cdk1/cyclin B1 in the regulation of MCAK, kinase assays *in vitro* were performed using purified His₆-tagged full-length MCAK as a substrate. As shown in Fig. 1A, Cdk1 readily phosphorylated recombinant MCAK and this phosphorylation was specific in a time- and dose-dependent manner (see Fig. S2A and B in the supplemental material). To narrow down the phosphorylated region, various GST-tagged structural domains of MCAK were subcloned. Among various domains, the core domain was found to be the major phosphorylated region in MCAK (Fig. 1B). This domain contains two residues, T537 and S566, which are conserved in human, mouse, rat, and *Xenopus* organisms (Fig. 1C), followed by a proline, minimal phosphorylation consensus site of Cdk1. To map the phosphorylation site, each potential phosphorylation site was replaced with alanine in the core domain of MCAK. In contrast to S566, mutation of T537 almost entirely abolished the phosphorylation signal (Fig. 1D). Finally, T537 was replaced with alanine in full-length MCAK. This mutant retained only 30% of the phosphorylation signal, relative to wild-type MCAK (Fig. 1E). These findings suggest that T537, which fits the complete phosphorylation consensus sequence (TPXR) of

Cdk1, is the major site of phosphorylation in the core domain of MCAK by Cdk1.

Phospho-specific antibodies specifically recognize phospho-T537 of MCAK *in vitro* and *in vivo*. To determine the function of the T537 phosphorylation of MCAK by Cdk1, phospho-specific antibodies were generated targeting the region surrounding phospho-T537 of MCAK (referred to hereafter as p-MCAK antibodies). To test the specificity of these antibodies, recombinant full-length MCAK and its various domains were incubated with active Cdk1 in the presence of nonradioactive ATP and subjected to Western blot analysis using p-MCAK antibodies. Only full-length MCAK and its core domain were recognized by p-MCAK antibodies in the presence of active Cdk1 (Fig. 2A, upper panel, lanes 1 and 7). To corroborate these data, full-length MCAK and its variant T537A were further subjected to kinase assays. While MCAK WT was readily phosphorylated by Cdk1 and detected by p-MCAK antibodies (Fig. 2B, top panels, lane 1), the replacement of T537 with alanine in full-length MCAK abolished this signal (Fig. 2B, top panels, lane 3), indicating that p-MCAK antibodies specifically recognize T537 phosphorylated by Cdk1. Moreover, to evaluate if phosphorylation of T537 in MCAK was dependent on Cdk1 activity, RO-3306, a selective small molecule inhibitor of Cdk1 (34), was used in kinase assays. In the presence of RO-3306, phosphorylation of full-length MCAK as well as its core domain was fully inhibited (see Fig. S3A, top panels, lanes 3 and 7, in the supplemental material).

To explore whether these p-MCAK specific antibodies could recognize phosphorylated MCAK *in vivo*, cellular extracts from mitotic HeLa cells were prepared for Western blot analysis with p-MCAK antibodies. Compared to control interphase extracts, mitotic extracts showed a band (Fig. 2C, top panel, lanes 1 and 2), which disappeared upon treatment with λ -phosphatase (data not shown). siRNA MCAK1 nearly abolished this signal, in comparison with control siRNA (Fig. 2C, top panel, lanes 3 and 5). Furthermore, siRNA targeting cyclin B1, the regulatory subunit of Cdk1, decreased the intensity of this band (Fig. 2C, top panel, lane 4). The results were further substantiated by showing that the Flag-tagged mutant MCAK T537A, expressed in HeLa cells, displayed only a weak signal (Fig. 2D, top panel, lane 3) relative to MCAK WT (Fig. 2D, top panel, lane 2). Finally, while mitotic extracts from HeLa cells showed this phospho-specific signal, lysates from mitotic HeLa 776-6 cells, in which the activity of Cdk1 is downregulated (40), did not exhibit this signal (see Fig. S3B, top panels, lanes 3 and 6, respectively, in the supplemental material).

We were further interested in the subcellular localization of the phosphorylated MCAK in cells. Interphase and mitotic HeLa cells were stained for phosphorylated MCAK, tubulin, and DNA. While interphase HeLa cells showed almost no staining (Fig. 2E, first row), mitotic HeLa cells exhibited strong phospho-signals at centrosomes, verified by centrosomal costaining of Polo-like kinase 1 (see Fig. S3C in the supplemental material), and in spindles (Fig. 2E, second and third rows). Weak signals could be also found in the cytoplasm. The phospho-staining in HeLa cells nearly disappeared upon treatment with siRNA against MCAK (Fig. 2E, fourth row) or cyclin B1 (Fig. 2E, last row). In addition, the phospho-MCAK was colocalized with cyclin B1 in mitosis (see Fig. S3D in the

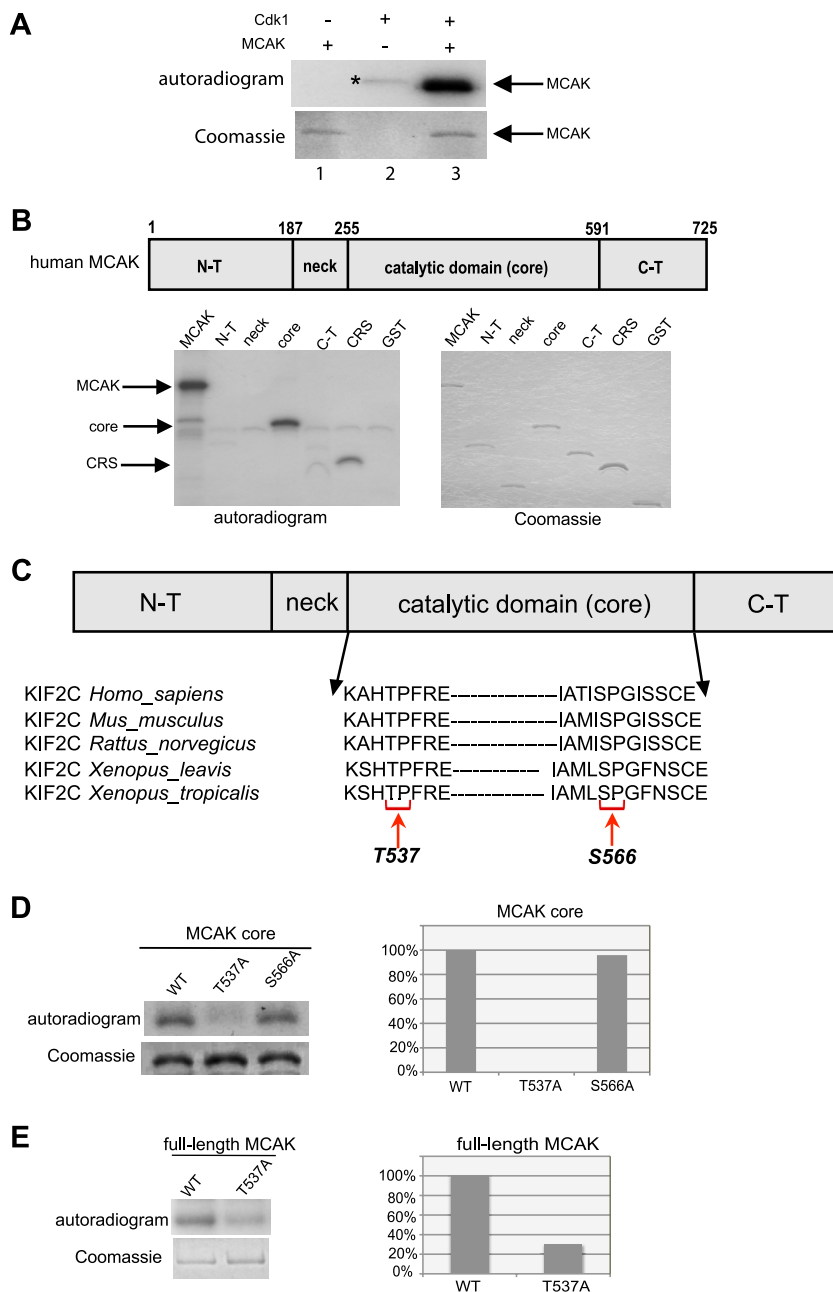
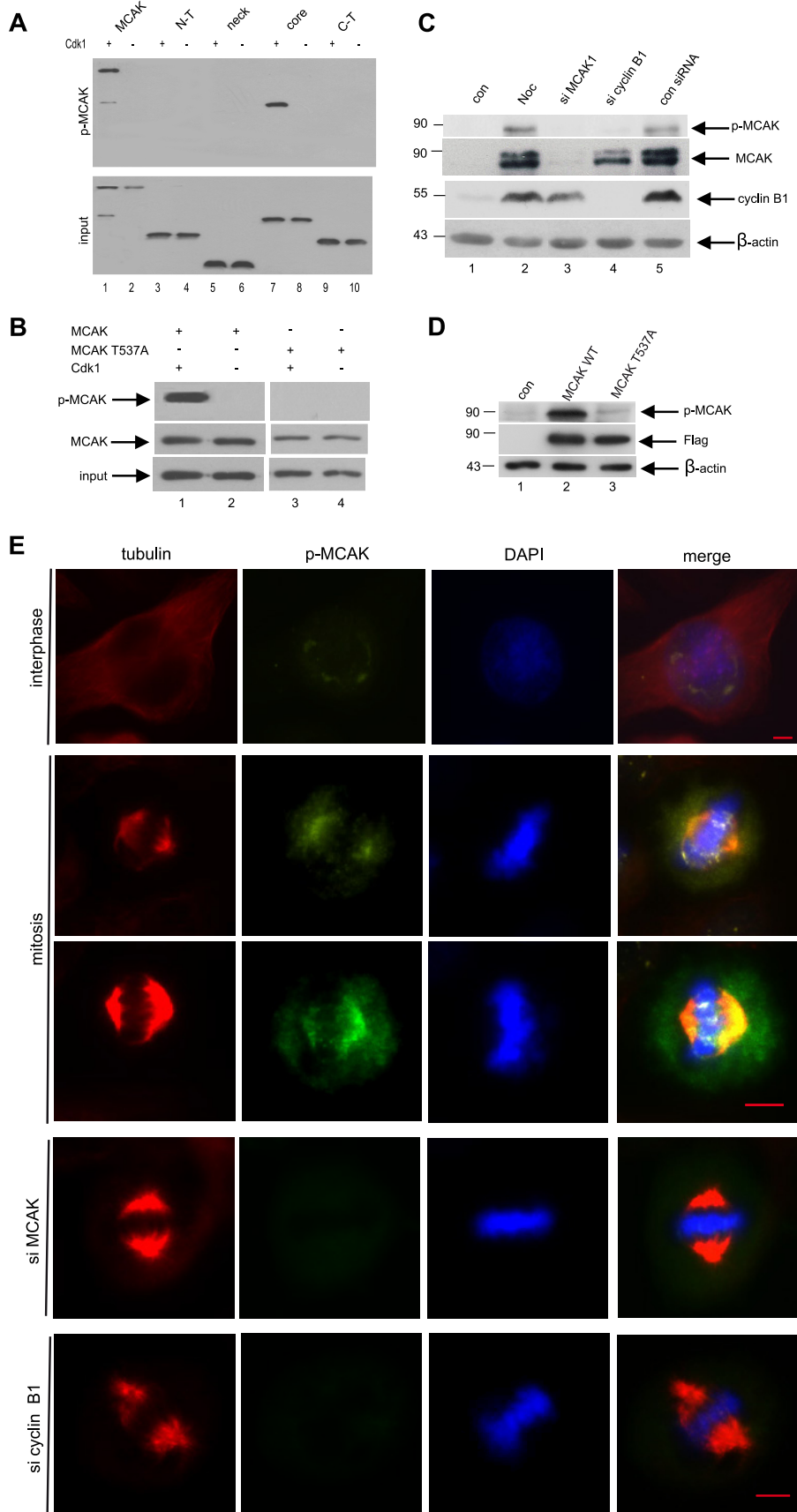


FIG. 1. Cdk1 phosphorylates T537 in the core domain of MCAK. (A) Purified His₆-tagged MCAK was subjected to kinase assays *in vitro* with active Cdk1/cyclin B1 (upper panel). *, autophosphorylated GST-cyclin B1. (B) (Upper panel) Schematic illustration of various domains of MCAK. (Lower panels) Kinase assays *in vitro* of GST-tagged MCAK domains with Cdk1/cyclin B1 (left panel). Cytoplasm retention signals (CRS) of cyclin B1 and GST proteins were taken as positive and negative controls, respectively. The same gel was stained with Coomassie blue as an input control (right panel). N-T, N terminus; C-T, C terminus. (C) Alignment of T537 and S566 in the catalytic core domain of MCAK in various species. (D) Kinase assays were performed using the GST-tagged core domain of MCAK and its mutants T537A and S566A, and the same gel was stained with Coomassie blue as an input control (left panel). Quantification of phospho-intensity, relative to the level for the input control (right panel). (E) Kinase assays of GST-tagged full-length MCAK, its mutant MCAK T537A, and the Coomassie blue staining control (left panel). Quantification of phospho-intensity, relative to the level for the input control (right panel).

supplemental material). The data strengthen the notion that this phosphorylation takes place in mitotic cells and is mediated by the activity of Cdk1/cyclin B1.

Phosphomimetic MCAK T537E attenuates its microtubule-destabilizing activity. To study the effect of phosphorylation of MCAK at T537 *in vitro*, His₆-tagged wild-type MCAK and its

variants T537A and T537E were expressed and purified. The ability of MCAK and its mutants to depolymerize microtubules was investigated using an *in vitro* depolymerization assay (9). Interestingly, MCAK T537E, the phosphomimetic MCAK variant, depolymerized microtubules more slowly than MCAK WT (Fig. 3A; see also Movies S1 to S3 in the supplemental



material). Moreover, MCAK T537A caused microtubule destabilization with kinetics very similar to that observed for MCAK WT, indicating that the alanine substitution does not alter the enzymatic activity of MCAK. The mean rates of depolymerization were 1.3, 1.2, and 0.3 $\mu\text{m}/\text{min}$ for MCAK WT, T537A, and T537E, respectively (Fig. 3A), suggesting that phosphorylation of MCAK by Cdk1 inhibits the ability of MCAK to depolymerize microtubules. In contrast, the ability of the variant T537E to hydrolyze ATP is not significantly altered relative to that of either the wild type or the T537A variant; the turnover rates for ATP hydrolysis are $0.78 \times 10^{-3} \pm 0.03 \times 10^{-3}$, $0.67 \times 10^{-3} \pm 0.06 \times 10^{-3}$, and $0.52 \times 10^{-3} \pm 0.09 \times 10^{-3}$ for T537E, T537A, and the wild type, respectively (data not shown). The lack of effect on ATP hydrolysis indicates that these mutations have not significantly disrupted the structure of the motor domain, thus suggesting that the observed decrease in microtubule depolymerization rate for the T537E variant is unlikely to be an artifact of misfolding of the motor domain caused by this point mutation. To address the destabilizing activity of MCAK WT and its mutants *in vivo*, as illustrated in Fig. 3B, HeLa cells were depleted of endogenous MCAK by use of siRNA MCAK2, which depletes only endogenous MCAK, as it corresponds to a sequence within the 3' untranslated region of the MCAK gene, and Flag-tagged MCAK plasmids and pBabe-puro constructs were added back on day 2. After selection with puromycin, cells were synchronized on days 3 and 4. Ten hours after release on day 5, the amounts of polymerized tubulin in transfected cells were evaluated (11, 31). In mitotic cells transfected with MCAK T537E, over 25% more polymerized tubulin was found than in cells transfected with MCAK WT or MCAK T537A (Fig. 3C), indicating that the microtubule-depolymerizing activity of MCAK is reduced by this mutation *in vivo*.

MCAK T537 mutants retain cells in prometaphase/metaphase. Overexpression or depletion of MCAK causes cells to sustain in prometaphase yet affects the mitotic indices only slightly (8, 10, 11, 44). We next investigated the functional significance of T537 phosphorylation in the regulation of mitosis. HeLa cells were treated as described in Fig. 3B. Endogenous MCAK was efficiently depleted (Fig. 4A, top panel, lane 3), and the expression levels of the various Flag-tagged MCAK constructs used were comparable (Fig. 4A, top panel, lanes 4 to 6). In parallel, treated cells were stained for DNA and phospho-histone H3, a mitotic marker, and positive cells in each group were quantified. We found that expression of MCAK

T537E or MCAK T537A induced a slight increase in the mitotic cell population, relative to the level for MCAK WT (Fig. 4B). Intriguingly, by further analyzing subphases of mitosis, we observed that MCAK T537A caused a 1.6-fold increase in prometaphase cells but that MCAK T537E induced a 1.4-fold increase in metaphase cells, relative to the levels for MCAK WT (Fig. 4C). These findings suggest that cells transfected with MCAK T537A confront a problem(s) already in prometaphase but that cells expressing MCAK T537E are able to go through prometaphase smoothly yet become disturbed in mitotic progression at the transition from metaphase to anaphase.

MCAK T537E induces displaced chromosomes, whereas MCAK T537A causes abnormal spindles. To explore the functional significance of phosphorylation of T537 in MCAK, we studied the phenotype of HeLa cells treated with siRNA MCAK2, which targets only endogenous MCAK. siRNA MCAK1, targeting both endogenous and exogenous MCAK, was used as a control. Both siRNAs worked efficiently (see Fig. S4A in the supplemental material). As expected, depletion of MCAK caused defects in chromosome positioning (Fig. 5A, and B, second row, DAPI). Moreover, mitotic spindle formation was also disrupted. In particular, prometaphase/metaphase cells frequently exhibited typical "hairy" spindles (Fig. 5B, second row, tubulin staining), comparable to earlier reports (8, 11, 33). In contrast, readdition of MCAK WT rescued the defect in chromosome positioning as well as abnormalities in the mitotic microtubule cytoskeleton induced by siRNA MCAK2 (Fig. 5B, third row) but not those induced by siRNA MCAK1 (Fig. 5A and data not shown).

Based on this rescue model, we asked whether MCAK T537E or MCAK T537A could substitute for endogenous MCAK as MCAK WT did. Cells were treated and synchronized to mitosis as illustrated in Fig. 3B, and chromosome behavior and spindle morphology in metaphase cells were examined by staining with α -tubulin antibodies and DAPI. Readdition of MCAK T537E caused obvious difficulty in chromosome positioning at the metaphase plate (Fig. 5C, DAPI). In particular, one or more chromosomes appeared to be around, rather than aligning properly at the spindle equator in metaphase. The frequency of metaphase cells with displaced chromosomes in 300 to 400 cells from each group was further microscopically quantified. While MCAK T537E caused a perturbation of chromosome position at the spindle equator by 3.5-fold over the level for MCAK WT (Fig. 5E), MCAK T537A was able to partially rescue this failure (Fig. 5E). While

FIG. 2. T537 phosphorylation takes place *in vivo* and is associated with Cdk1 activity. (A) GST-tagged full-length MCAK, the N terminus, the neck region, the core domain, and the C terminus were subjected to kinase assays with or without Cdk1 in the presence of nonradioactive ATP. The reactions were subjected to Western blot analysis with phospho-antibodies against phospho-T537 of MCAK (p-MCAK; upper panel). The same membrane was further probed with GST antibodies as an input control (lower panel). (B) GST-tagged full-length MCAK WT or its mutant MCAK T537A was taken as a substrate for kinase assays with or without Cdk1 in the presence of nonradioactive ATP. The reactions were further analyzed with Western blot analysis using p-MCAK and MCAK antibodies. The same membrane was probed with GST antibodies as an input control. (C) HeLa cells were transfected with control siRNA or siRNA targeting MCAK or cyclin B1 and then synchronized to prometaphase. Lysates were prepared for Western blot analyses using p-MCAK antibodies (top panel), MCAK antibodies (second panel), cyclin B1 (third panel), or β -actin (bottom panel). con, control extracts from nonsynchronized cells. (D) HeLa cells were transfected with Flag-tagged MCAK WT or MCAK T537A and synchronized to prometaphase. Western blot analyses were performed with p-MCAK antibodies. The same membrane was further stained with antibodies against the Flag tag and β -actin for transfection efficiency and loading control, respectively. con, control extracts from nonsynchronized cells. (E) Immunofluorescence staining. HeLa cells were stained for tubulin, phospho-MCAK, and DAPI. Representatives of HeLa cells observed in interphase (first row), observed in mitosis (second and third rows), or treated with siRNA targeting MCAK (fourth row) or cyclin B1 (last row) are illustrated. Bar, 5 μm .

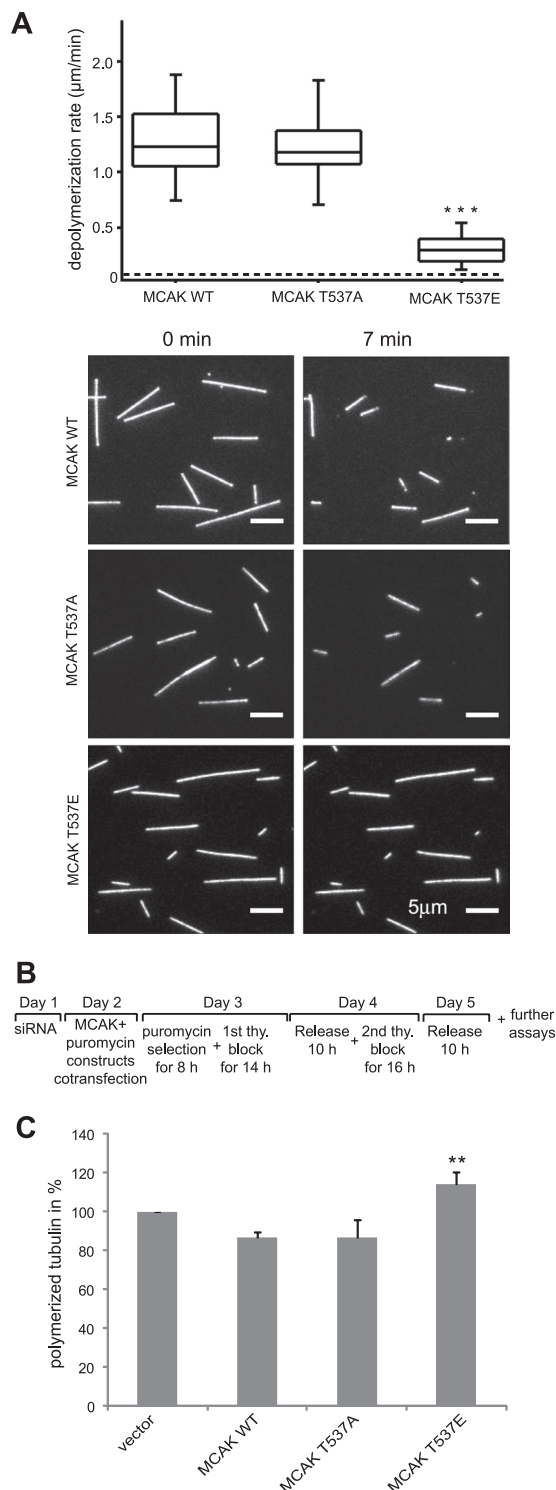


FIG. 3. Phosphomimetic MCAK T537E attenuates its microtubule-destabilizing activity *in vitro* as well as *in vivo*. (A) *In vitro* depolymerization assays. (Upper panel) Box plots depicting the distribution of depolymerization rates of individual microtubules observed upon addition of MCAK WT ($n = 45$), MCAK T537A ($n = 44$), or MCAK T537E ($n = 59$). The box depicts the range between the 1st and 3rd quartiles (i.e., central 50% of the distribution), with the central line showing the position of the median. ***, $P < 0.001$. The dashed line shows the spontaneous depolymerization rate for the stabilized microtubules used in these assays ($0.03 \mu\text{m}/\text{min}$). (Lower panel) Represent

most cells with MCAK T537E displayed almost normal bipolar spindle assembly (Fig. 5C, tubulin staining), the ability of cells expressing MCAK T537A to form a normal mitotic spindle was dramatically compromised: the microtubule cytoskeleton appeared as two dense, star-like asters, and most microtubules near the chromosome region were absent (Fig. 5D, tubulin staining). Thus, the defect in spindle formation might account for the retention of cells expressing MCAK T537A in prometaphase, whereas the failure of chromosome positioning causes a metaphase block in cells transfected with MCAK T537E (Fig. 4C). We could not observe an obvious defect in chromosome segregation by lagging chromosome in anaphase. However, it is possible that we missed the time window.

Intercentromere distance is reduced in HeLa cells expressing MCAK T537E. As phosphorylation of T537 attenuated its microtubule-destabilizing ability (Fig. 3), we hypothesized that phosphomimetic MCAK T537E might fail to correct inappropriate microtubule-kinetochore attachments and to generate tension between sister kinetochores/centromeres in metaphase, leading to a decrease in intercentromere distance. To test this, Flag-tagged MCAK WT and its mutant constructs were transfected into HeLa cells depleted of endogenous MCAK. Cells were synchronized to mitosis and then stained for centromere marker Cenp-A and α -tubulin. A clear decrease in intercentromere distance was observed in HeLa cells expressing MCAK T537E (Fig. 6A, last row), relative to the level for HeLa cells transfected with MCAK WT (Fig. 6A, second row). As expected, depletion of MCAK reduced this distance (Fig. 6A, first row). Interestingly, those MCAK T537A transfected cells, which were able to reach metaphase, also displayed a reduced intercentromere distance (Fig. 6A, third row), indicating that the unphosphorylatable form MCAK T537A is incapable of fulfilling its function within cells despite its active microtubule-destabilizing activity (Fig. 3). This is possibly due to an alteration in its subcellular localization relative to that of the wild-type protein (see below). Further quantification revealed that the average distances of intercentromeres were $1.5 \mu\text{m}$, $1.1 \mu\text{m}$, and $0.9 \mu\text{m}$ in HeLa cells expressing MCAK WT, MCAK T537A, and MCAK T537E, respectively (Fig. 6B). These data imply that interfering with phosphorylation of T537 in the core domain of MCAK perturbs the generation of local tension and concomitantly deregulates correction of improper microtubule attachments.

Cdk1 controls the centrosomal localization of MCAK. To investigate if phosphorylation of T537 in MCAK affects the subcellular localization of MCAK, HeLa cells, which expressed

tative epifluorescence images of immobilized microtubules either prior to or 7 min after addition of MCAK WT, T537A, or T537E. Bar, $5 \mu\text{m}$. (B) Working schedule. (C) Quantification of polymerized tubulin content *in vivo*. HeLa cells were transfected with Flag-tagged MCAK WT, its mutants, or empty vector in an endogenous MCAK-depleted background. Transfected cells were then synchronized to the G_1/S boundary and released for 10 h. Cellular polymerized tubulin contents were analyzed by flow cytometry after cells were extracted, fixed, and stained for tubulin. The amount of polymerized tubulin from Flag vector plasmid-transfected HeLa cells was assigned as 100%. The results are presented as means \pm standard deviations (SD) ($n = 3$). **, $P < 0.01$ for comparison to MCAK WT.

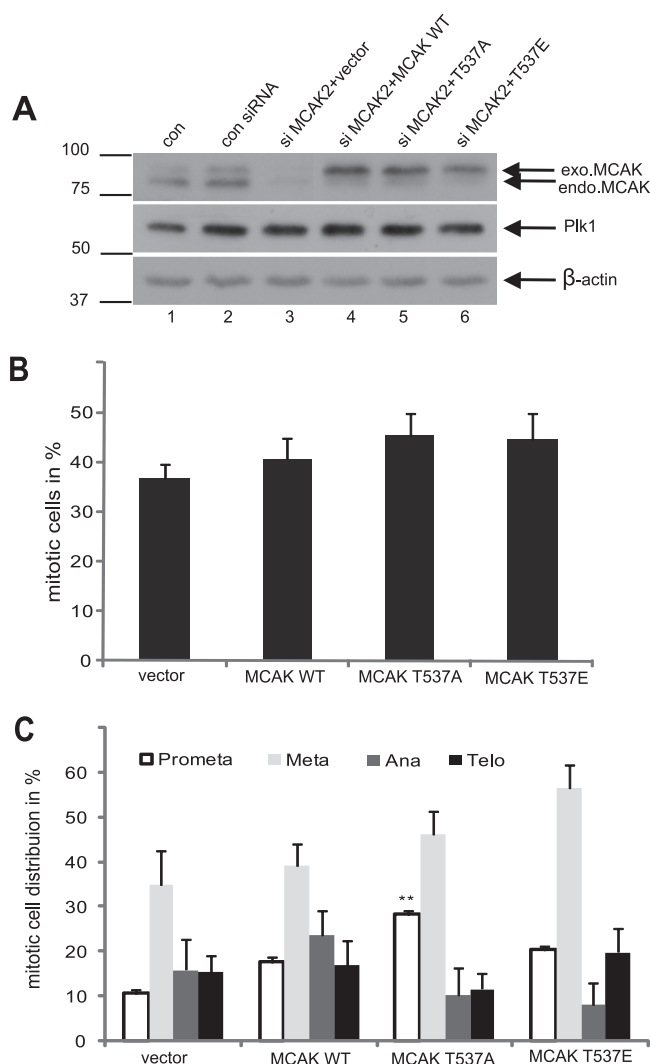


FIG. 4. Interfering with T537 in MCAK causes cells to be retained in prometaphase/metaphase. (A) Western blot analysis. HeLa cells were transfected with Flag-tagged MCAK WT, MCAK T537A, MCAK T537E, or Flag vector after depletion of endogenous MCAK with siRNA MCAK2, synchronized to the G₁/S boundary, and released for 10 h. Western blot analyses were carried out with MCAK antibodies (top panel), Plk1 antibodies (mitotic control; middle panel), and β-actin antibodies as a loading control (bottom panel). Extracts from nontransfected and nonsynchronized cells (con) and control siRNA-treated and synchronized cells (con siRNA) were taken as controls. (B) Mitotic indices. Treated cells were stained for phospho-histone H3 (S10) and DNA, and mitotic indices were scored by microscopy. The results are presented as means ± SD. (C) The percentages of mitotic subphases were further analyzed. The results are presented as means ± SD, statistically analyzed, relative to the level for the vector control. **, *P* < 0.01.

comparable levels of enhanced green fluorescent protein (EGFP)-tagged MCAK or its mutants (see Fig. S4B in the supplemental material), were stained for tubulin, phospho-MCAK, and DNA. In mitotic cells, in which EGFP-tagged MCAK WT was diffusely localized at centrosomes and mitotic spindles, the phospho-staining was readily detectable (Fig. 7A, first row) and was colocalized with cyclin B1 (see Fig. S3D in the supplemental material). Intriguingly, in mitotic cells, in

which EGFP-tagged MCAK WT was strongly bound to the metaphase plate (as in Fig. 7B, first row), the phospho-signal was hardly observed (data not shown), indicating that phosphorylation of MCAK by Cdk1 is possibly catalyzed by phosphatases as soon as the phosphorylated MCAK arrives at the equatorial plate. Furthermore, EGFP-tagged MCAK WT turned out to be accumulated at centrosomes upon depletion of cyclin B1, along with remarkably reduced phospho-signal (Fig. 7A, second row). In line with the observation and regardless of the presence of cyclin B1, MCAK T537A was predominantly found to be at centrosomes in prometaphase/metaphase cells (Fig. 7A, third and fourth rows), which was confirmed by pericentrin staining that overlapped with EGFP-tagged MCAK T537A (see Fig. S4C in the supplemental material). The phospho-signal in HeLa cells with MCAK T537A resulted from the endogenous MCAK phosphorylated by Cdk1, as downregulation of cyclin B1 almost abolished this phospho-staining (Fig. 7A, p-MCAK staining in third and fourth rows). Moreover, HeLa cells transfected with MCAK T537A displayed two star-like mitotic spindles with deviant spindles (Fig. 7A, fourth row, tubulin staining). As for MCAK T537E, it was to be found at the equatorial plate, in addition to the distribution at centrosomes and spindles (Fig. 7A, fifth row). Unlike MCAK WT (Fig. 7A, second row), EGFP-tagged MCAK T537E almost kept its distribution and was not changed to centrosomes upon depletion of cyclin B1 (Fig. 7A, last row). Further microscopic analysis of 300 to 400 transfected prometaphase/metaphase cells in each group revealed that the percentages of the concentrated centrosomal localization of EGFP-tagged MCAK WT, MCAK T537E, and MCAK T537A were 4%, 14%, and 65%, respectively. The enhanced centrosomal localization of MCAK T537A was also observed in the colon cancer SW-480 cell line (data not shown).

To further substantiate that MCAK's centrosomal localization was linked to the Cdk1 activity, both control HeLa cells and HeLa 776-6 cells, in which the activity of Cdk1 is down-regulated by depletion of cyclin B1 (40), were transfected with EGFP-tagged MCAK WT. Unlike in control HeLa cells (Fig. 7B, top row), MCAK WT was preferentially localized at centrosomes in HeLa 776-6 cells, which is also accompanied by formation of aberrant spindles (Fig. 7B, bottom row). These data provide the evidence that Cdk1 affects the localization of MCAK in mitosis, and the enhanced centrosomal localization of MCAK is related to the reduced activity of Cdk1.

DISCUSSION

Regulation of MCAK on the centromeres/kinetochores by Aurora B kinase has been well studied (1, 18, 28, 29, 43). We show here that unlike Aurora B, Cdk1 phosphorylates one threonine residue in the core domain of MCAK *in vitro* and *in vivo*, which regulates the microtubule-destabilizing activity and subcellular localization of MCAK. Interfering with the regulation of MCAK by Cdk1 causes dramatic defects in mitosis in human cells.

Phosphorylation of T537 in the core domain of MCAK attenuates the microtubule-destabilizing activity of MCAK *in vitro* and *in vivo* (Fig. 3). T537 is located in the L12 loop of the MCAK core domain, which is immediately C-terminal to the α4 helix of the core domain in MCAK. It has been suggested

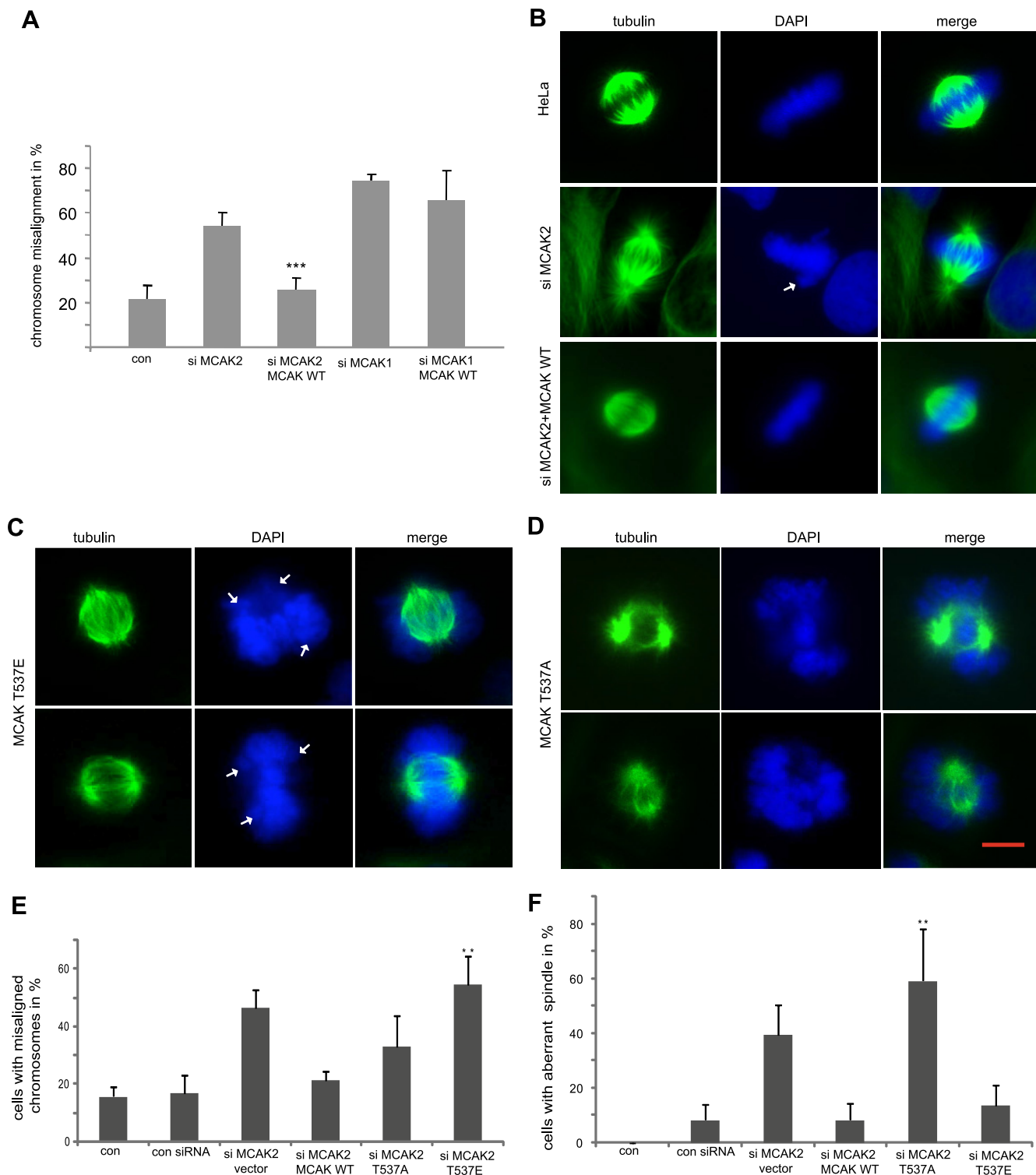


FIG. 5. MCAK T537E induces displaced chromosomes, whereas MCAK T537A causes abnormal spindles. (A) Rescue model. HeLa cells were treated with siRNA MCAK2 against only endogenous MCAK, followed by readdition of Flag-tagged MCAK WT. Cells were synchronized to the G₁/S boundary and released for 10 h. Cells with displaced chromosomes in mitotic cells stained with α -tubulin and DAPI were quantified. The results are presented as means \pm SD, statistically analyzed. ***, $P < 0.001$. siRNA MCAK1 treatment alone and readdition of MCAK WT served as controls, as siRNA MCAK1 is targeting both endogenous and exogenous MCAK. (B) Examples of control mitotic HeLa cells (top row), HeLa cells depleted of endogenous MCAK (middle row), and HeLa cells with readdition of Flag-tagged MCAK WT after depletion of endogenous MCAK (bottom row). Arrowhead, displaced chromosome. (C) Representatives of HeLa cells transfected with MCAK T537E after depletion of endogenous MCAK. Arrowhead, displaced chromosome. (D) Examples of HeLa cells transfected with MCAK T537A after depletion of endogenous MCAK. Bar, 5 μ m. (E) The percentages of chromosome mispositioning were microscopically evaluated. The results are presented as means \pm SD, statistically analyzed. **, $P < 0.01$. (F) Frequencies of cells with abnormal spindle formation. The results are presented as means \pm SD, statistically analyzed. **, $P < 0.01$.

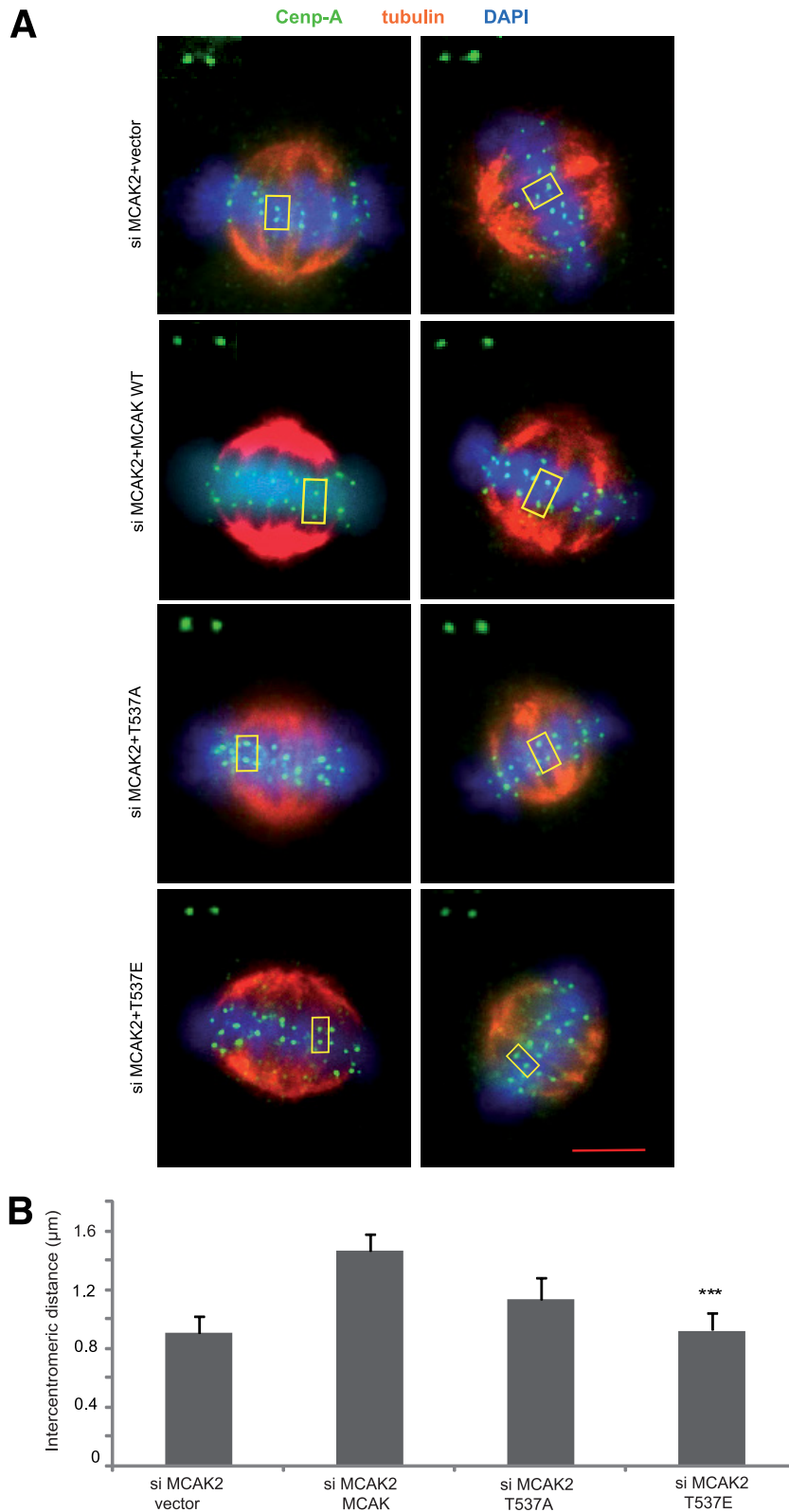
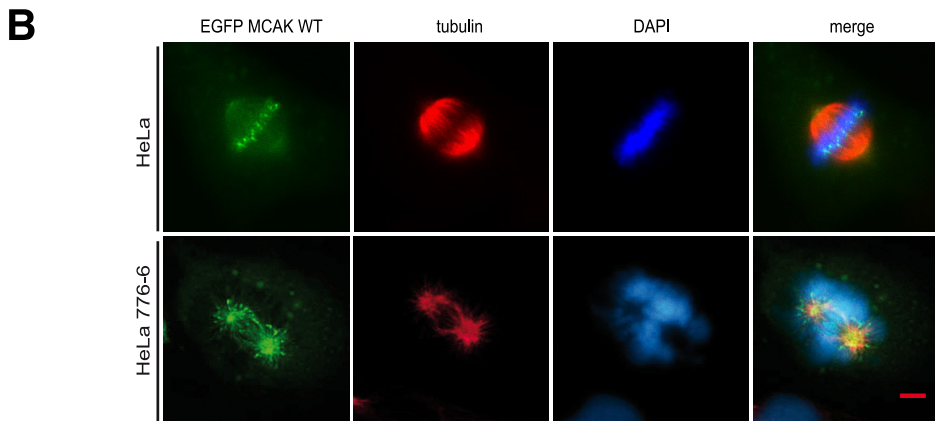
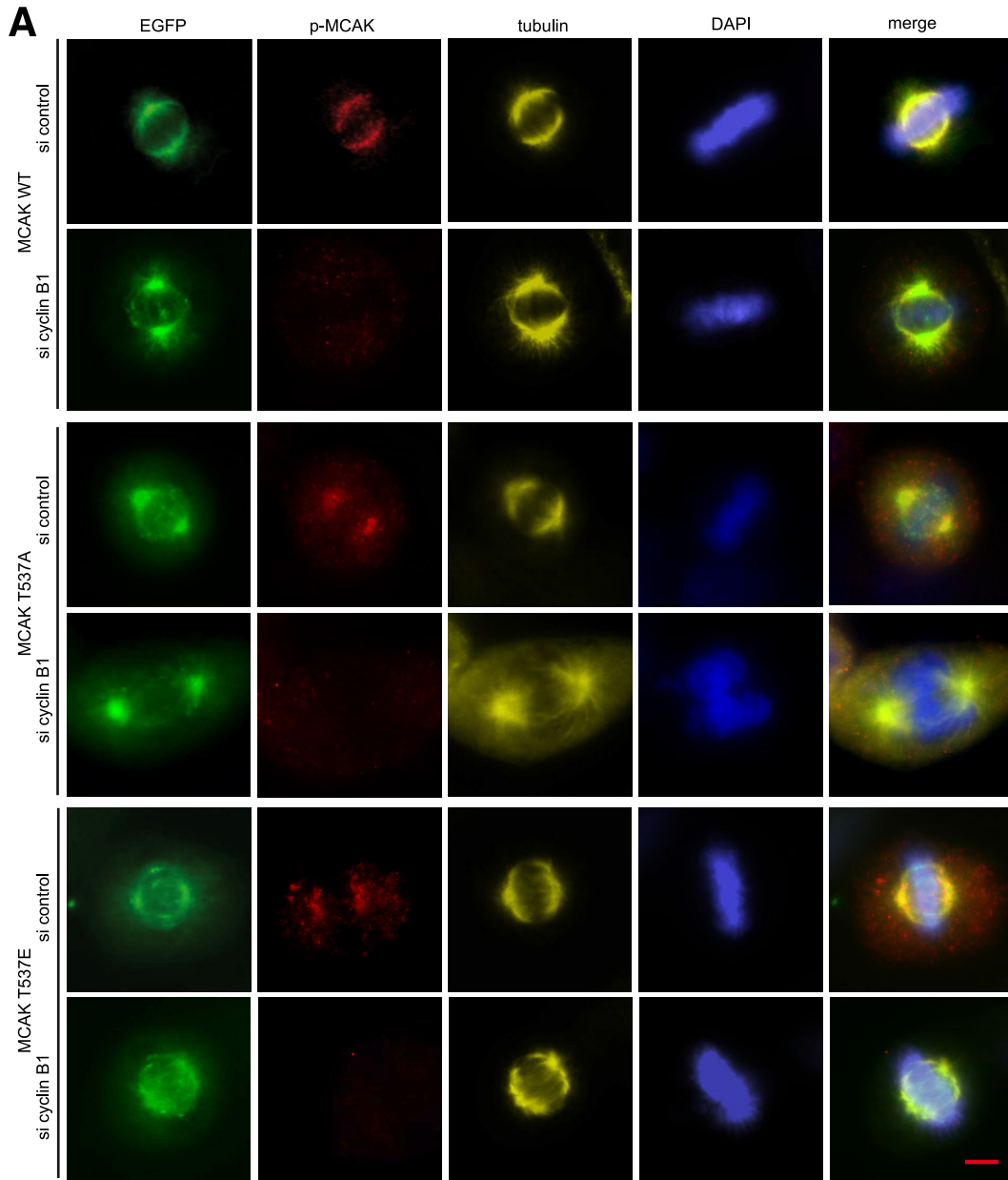


FIG. 6. Mutation of T537 of MCAK results in a reduced distance of intercentromeres. HeLa cells depleted of endogenous MCAK were transfected with either control Flag vector, MCAK WT, or its mutants, synchronized to the G₁/S boundary, and released for 10 h. Cells were then stained for Cenp-A, a centromere marker, and α -tubulin. Intercentromeric distances were measured as described in Materials and Methods. (A) Examples of HeLa cells transfected with vector, MCAK WT, MCAK T537A, or MCAK T537E. Bar, 5 μ m. Insets show representative sister centromeres. (B) The percentages of the average intercentromeric distances of metaphase cells rescued with vector, MCAK WT, MCAK T537A, or MCAK T537E. The results are presented as means \pm SD, statistically analyzed. ***, $P < 0.001$.



that the $\alpha 4$ helix is directly involved in binding to the curved conformation of tubulin at the ends of microtubule protofilaments and thereby facilitates depolymerization (26). It is therefore possible that the introduction of a negative charge via phosphorylation of the residue T537, which is in the region adjacent to the $\alpha 4$ helix, could disrupt the interaction of MCAK with the microtubule end, therefore leading to the attenuation of the microtubule-destabilizing activity of MCAK. T537 in the motor domain is conserved in human, mouse, rat, and *Xenopus* organisms, suggesting a general regulatory mechanism in high species. It is also interesting to note that a close phosphorylation site (S573) in the motor domain of *Drosophila* kinesin 13 is phosphorylated, controlling the time and place of microtubule depolymerization (23).

In the *Xenopus* egg extract system, MCAK is vital for controlling microtubule dynamics, as demonstrated by the long microtubules that organize into large sunburst arrays upon its removal (36). Since cytoplasmic control of microtubule polymerization does not require Aurora B-mediated inhibition of MCAK, Cdk1/cdc2 has been proposed to be responsible for this process (28). In this work, we show that Cdk1-mediated phosphorylation of MCAK, being mostly found at the spindle poles (Fig. 2E), is required for proper spindle assembly during mitosis in human cells. In cells expressing MCAK T537A, a form unphosphorylatable by Cdk1, mitotic spindles appeared abnormal and microtubules were sparse near the chromosome region (Fig. 5D and 7A), indicative of excessive MCAK activity promoting microtubule catastrophe (10, 30). This is underlined by the observation that HeLa 776-6 cells with reduced Cdk1 activity very often display defects in spindle assembly (Fig. 7B). In contrast, cells expressing the phosphomimetic MCAK T537E, which has a reduced microtubule-destabilizing activity, exhibit almost normal mitotic spindle formation (Fig. 5C). These data suggest that phosphorylation of MCAK by Cdk1 is required for proper spindle formation in mitosis since this phosphorylation inhibits the microtubule-destabilizing ability of MCAK.

While phosphorylation of MCAK by Cdk1 has been shown to be required for the proper assembly of mitotic spindle in early mitosis, subsequent dephosphorylation of T537 and/or additional modifications of MCAK by other regulators appear to be necessary for correct chromosome positioning at the metaphase plate. The addition of MCAK WT can rescue defects in chromosome positioning in MCAK-depleted cells, whereas readdition of the phosphomimetic MCAK T537E is not able to restore such defects (Fig. 5C and E), indicating that phosphorylation of MCAK by Cdk1 compromises the ability of MCAK to correct erroneous microtubule-kinetochore attachments and possibly also reduces the tension at the sister centromeres/kinetochores by perturbed control over microtubule

dynamics. This notion is supported by decreased intercentromere distances observed in mitotic cells expressing MCAK T537E (Fig. 6). Notably, cells rescued with MCAK T537A also show a compromised intercentromere distance (Fig. 6), which could possibly be explained by its main localization at centrosomes (Fig. 7A). Thus, sustained phosphorylation of MCAK by Cdk1 hampers the function of MCAK, and timely dephosphorylation of MCAK around the centromeres/kinetochores is required for proper chromosome positioning at the metaphase plate and smooth progression of mitosis.

Furthermore, regulation of MCAK by Cdk1 influences the subcellular localization of MCAK. MCAK was originally identified as a protein that localizes to the centromeres, where it corrects improper kinetochore-microtubule attachments in mitosis (14, 36, 38). A recent study has proposed that the localization of MCAK on chromosome arms, centromeres, and kinetochores is spatially and temporally regulated by Aurora B kinase during mitosis (43). The work described here highlights that phosphorylation of MCAK by Cdk1 modulates the localization of MCAK at centrosomes: like the unphosphorylatable MCAK T537A, MCAK WT turns out to be preferentially concentrated at centrosomes upon depletion of cyclin B1 (Fig. 7A). Moreover, the phosphomimetic MCAK T537E is diffusely distributed at the spindle poles and the metaphase plate and is not changed to centrosomes after depletion of cyclin B1 (Fig. 7A). This argument is further strengthened by the observation that MCAK is accumulated at centrosomes in HeLa 776-6 cells with downregulated Cdk1 activity (Fig. 7B). Remarkably, the phospho-signal is found only at centrosomes and the spindle and is hardly detectable at the metaphase plate (Fig. 7A), indicating that phosphorylation of MCAK by Cdk1 takes place at the spindle poles. It is thus tempting to suggest that phosphorylation of MCAK by Cdk1 in early mitosis functions as a switch driving the release of MCAK from the spindle poles to other cellular locations, thereby allowing spindle nucleation and formation.

On the basis of our data, we propose a model of how Cdk1 might regulate MCAK in mitosis (Fig. 8). In early mitosis, phosphorylation of MCAK by Cdk1 promotes the release of MCAK from the spindle poles and facilitates mitotic spindle formation (Fig. 8B, top row). In metaphase, dephosphorylation of MCAK around the centromeres/kinetochores and/or further modifications by other kinases, such as Aurora B, take over the functional control of MCAK in correcting malattachments of microtubule-kinetochore (Fig. 8B, top row). While MCAK T537A localizes preferentially to centrosomes and induces extreme defects in spindle formation (Fig. 8B, middle row), MCAK T537E raises dramatic defects in chromosome positioning at the metaphase plate (Fig. 8B, bottom row). Thus, Cdk1 is an important regulator for the function and localiza-

FIG. 7. Phosphorylation of T537 releases MCAK from centrosomes. (A) HeLa cells were treated with control siRNA or siRNA cyclin B1 on day 1 and were transfected with EGFP-tagged MCAK WT, MCAK T537A, or MCAK T537E on day 2. Cells were then synchronized to the G₁/S boundary. Ten hours after release, cells were stained for phosphorylated MCAK (p-MCAK), α -tubulin, and DNA. Examples of mitotic HeLa cells transfected with MCAK WT (first two rows), MCAK T537A (third and fourth rows), or MCAK T537E (last two rows), either treated with control siRNA (si control) or treated with siRNA cyclin B1 (si cyclin B1), as indicated, are depicted. Bar, 5 μ m. (B) Control HeLa cells or HeLa 776-6 cells, in which the Cdk1 activity is downregulated by depleting cyclin B1, were transfected with EGFP-tagged MCAK WT. Cells were synchronized to the G₁/S boundary. Ten hours after release, cells were stained for α -tubulin and DNA. Representatives of HeLa or HeLa 776-6 cells transfected with EGFP-MCAK WT are shown. Bar, 5 μ m.

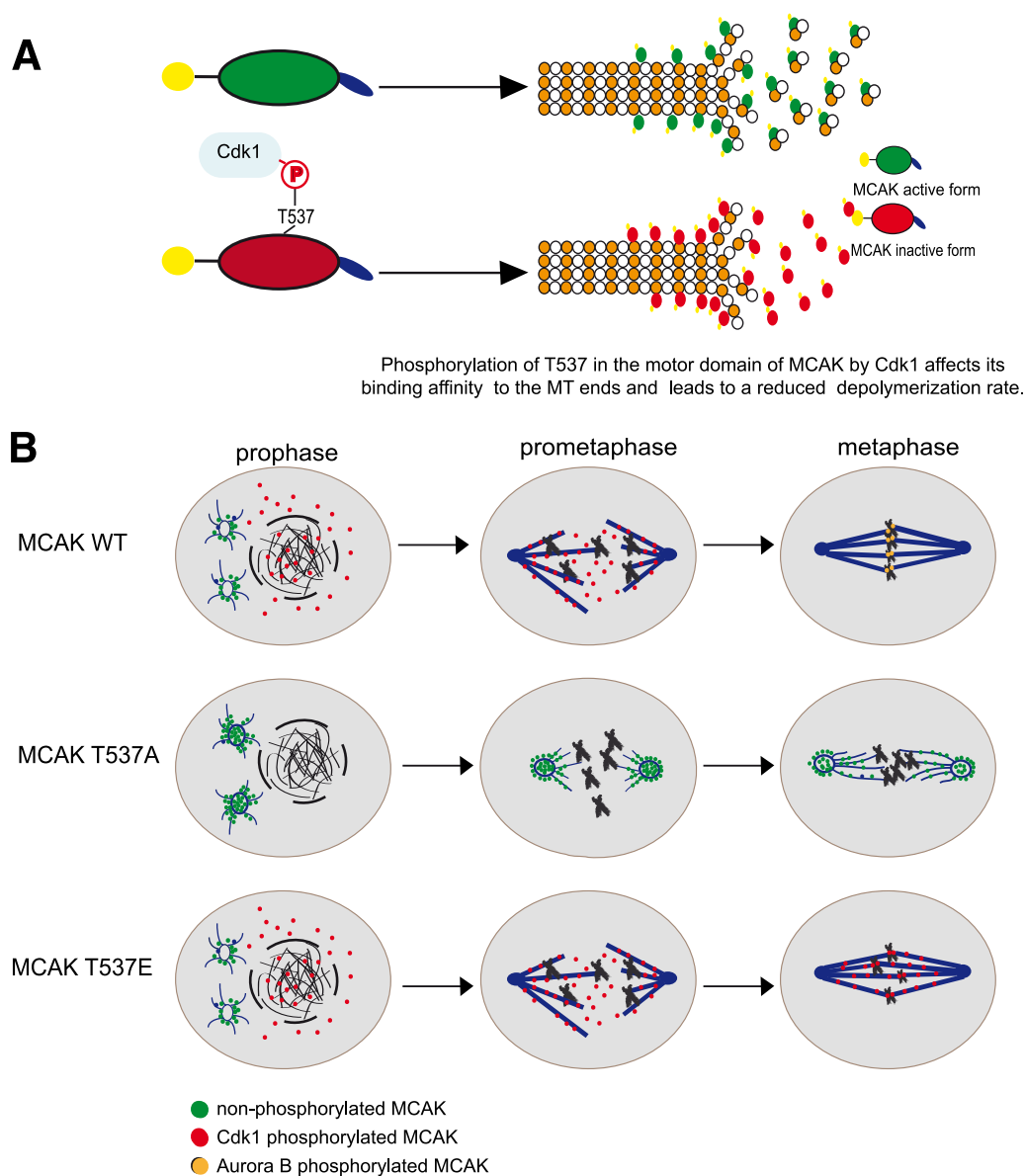


FIG. 8. Schematic illustration of the regulation of MCAK by Cdk1. (A) Cdk1 phosphorylates T537 in the core domain of MCAK and attenuates the catalytic activity of MCAK. (B) Phosphorylation by Cdk1 releases MCAK from the spindle poles and promotes the spindle assembly by inhibiting the activity of MCAK in prophase/prometaphase. To restore the activity of MCAK, dephosphorylation of T537 around the centrosomes/kinetochores in metaphase takes place to ensure the function of MCAK in correcting improper kinetochore-microtubule attachments, mainly controlled by Aurora B kinase (top row). Therefore, MCAK T537A, the unphosphorylatable form of MCAK, localizes preferentially to centrosomes and induces aberrant spindle formation (middle row), whereas MCAK T537E, the constitutive phosphomimetic form, generates defects in chromosome positioning (bottom row).

tion of MCAK in mitosis. This regulation of MCAK by Cdk1 coordinates with and fine-tunes the regulation of MCAK by Aurora B to ensure the correct temporal and spatial control over MCAK. Further investigations are warranted to elucidate the precise sequence of regulatory events orchestrated by Cdk1 and Aurora B in the context of the localization, enzymatic activity, and overall function of MCAK during mitosis.

ACKNOWLEDGMENTS

This work is supported by Deutsche Krebshilfe (numbers 107594 and 108553).

We are grateful to M. Gullberg, Department of Molecular Biology, Umeå University, Umeå, Sweden, for his critical reading of the manuscript and for the detailed protocol for the measurement of cellular microtubule polymer content. We extend our great thanks to H. Eichenlaub-Ritter, Faculty of Biology, Gene Technology/Microbiology, University of Bielefeld, Bielefeld, Germany, for critical reading of the manuscript.

REFERENCES

- Andrews, P. D., Y. Ovechkina, N. Morrice, M. Wagenbach, K. Duncan, L. Wordeman, and J. R. Swedlow. 2004. Aurora B regulates MCAK at the mitotic centromere. *Dev. Cell* 6:253–268.
- Bentley, A. M., G. Normand, J. Hoyt, and R. W. King. 2007. Distinct se-

- quence elements of cyclin B1 promote localization to chromatin, centrosomes, and kinetochores during mitosis. *Mol. Biol. Cell* **18**:4847–4858.
3. Cassimeris, L., and J. Morabito. 2004. TOGp, the human homolog of XMAP215/Dis1, is required for centrosome integrity, spindle pole organization, and bipolar spindle assembly. *Mol. Biol. Cell* **15**:1580–1590.
 4. Chen, Q., X. Zhang, Q. Jiang, P. R. Clarke, and C. Zhang. 2008. Cyclin B1 is localized to unattached kinetochores and contributes to efficient microtubule attachment and proper chromosome alignment during mitosis. *Cell Res.* **18**:268–280.
 5. De Luca, M., L. Brunetto, I. A. Asteriti, M. Giubettini, P. Lavia, and G. Guarguaglini. 2008. Aurora-A and ch-TOG act in a common pathway in control of spindle pole integrity. *Oncogene* **27**:6539–6549.
 6. Desai, A., S. Verma, T. J. Mitchison, and C. E. Walczak. 1999. Kin I kinesins are microtubule-destabilizing enzymes. *Cell* **96**:69–78.
 7. Ganem, N. J., and D. A. Compton. 2004. The KinI kinesin Kif2a is required for bipolar spindle assembly through a functional relationship with MCAK. *J. Cell Biol.* **166**:473–478.
 8. Hedrick, D. G., J. R. Stout, and C. E. Walczak. 2008. Effects of anti-microtubule agents on microtubule organization in cells lacking the kinesin-13 MCAK. *Cell Cycle* **7**:2146–2156.
 9. Helenius, J., G. Brouhard, Y. Kalaidzidis, S. Diez, and J. Howard. 2006. The depolymerizing kinesin MCAK uses lattice diffusion to rapidly target microtubule ends. *Nature* **441**:115–119.
 10. Holmfeldt, P., S. Stenmark, and M. Gullberg. 2004. Differential functional interplay of TOGp/XMAP215 and the KinI kinesin MCAK during interphase and mitosis. *EMBO J.* **23**:627–637.
 11. Holmfeldt, P., X. Zhang, S. Stenmark, C. E. Walczak, and M. Gullberg. 2005. CaMKIIγ-mediated inactivation of the Kin I kinesin MCAK is essential for bipolar spindle formation. *EMBO J.* **24**:1256–1266.
 12. Howard, J., and A. A. Hyman. 2007. Microtubule polymerases and depolymerases. *Curr. Opin. Cell Biol.* **19**:31–35.
 13. Huang, H., J. Feng, J. Famulski, J. B. Rattner, S. T. Liu, G. D. Kao, R. Muschel, G. K. Chan, and T. J. Yen. 2007. Tripin/hSgo2 recruits MCAK to the inner centromere to correct defective kinetochore attachments. *J. Cell Biol.* **177**:413–424.
 14. Kline-Smith, S. L., A. Khodjakov, P. Hergert, and C. E. Walczak. 2004. Depletion of centromeric MCAK leads to chromosome congression and segregation defects due to improper kinetochore attachments. *Mol. Biol. Cell* **15**:1146–1159.
 15. Kline-Smith, S. L., and C. E. Walczak. 2002. The microtubule-destabilizing kinesin XKCM1 regulates microtubule dynamic instability in cells. *Mol. Biol. Cell* **13**:2718–2731.
 16. Knowlton, A. L., W. Lan, and P. T. Stukenberg. 2006. Aurora B is enriched at merotelic attachment sites, where it regulates MCAK. *Curr. Biol.* **16**:1705–1710. doi:S0960-9822(06)01962-2.
 17. Kreis, N. N., K. Sommer, M. Sanhaji, A. Kramer, Y. Matthes, M. Kaufmann, K. Strebhardt, and J. Yuan. 2009. Long-term downregulation of Polo-like kinase 1 increases the cyclin-dependent kinase inhibitor p21(WAF1/CIP1). *Cell Cycle* **8**:460–472.
 18. Lan, W., X. Zhang, S. L. Kline-Smith, S. E. Rosasco, G. A. Barrett-Wilt, J. Shabanowitz, D. F. Hunt, C. E. Walczak, and P. T. Stukenberg. 2004. Aurora B phosphorylates centromeric MCAK and regulates its localization and microtubule depolymerization activity. *Curr. Biol.* **14**:273–286.
 19. Lawrence, C. J., R. K. Dawe, K. R. Christie, D. W. Cleveland, S. C. Dawson, S. A. Endow, L. S. Goldstein, H. V. Goodson, N. Hirokawa, J. Howard, R. L. Malmberg, J. R. McIntosh, H. Miki, T. J. Mitchison, Y. Okada, A. S. Reddy, W. M. Saxton, M. Schliwa, J. M. Scholey, R. D. Vale, C. E. Walczak, and L. Wordeman. 2004. A standardized kinesin nomenclature. *J. Cell Biol.* **167**:19–22.
 20. Malumbres, M., and M. Barbacid. 2009. Cell cycle, CDKs and cancer: a changing paradigm. *Nat. Rev. Cancer* **9**:153–166.
 21. Maney, T., A. W. Hunter, M. Wagenbach, and L. Wordeman. 1998. Mitotic centromere-associated kinesin is important for anaphase chromosome segregation. *J. Cell Biol.* **142**:787–801.
 22. Maney, T., M. Wagenbach, and L. Wordeman. 2001. Molecular dissection of the microtubule depolymerizing activity of mitotic centromere-associated kinesin. *J. Biol. Chem.* **276**:34753–34758.
 23. Mennella, V., D. Y. Tan, D. W. Buster, A. B. Asenjo, U. Rath, A. Ma, H. J. Sosa, and D. J. Sharp. 2009. Motor domain phosphorylation and regulation of the *Drosophila* kinesin 13, KLP10A. *J. Cell Biol.* **186**:481–490.
 24. Moore, A., and L. Wordeman. 2004. The mechanism, function and regulation of depolymerizing kinesins during mitosis. *Trends Cell Biol.* **14**:537–546.
 25. Nakamura, Y., F. Tanaka, N. Haraguchi, K. Mimori, T. Matsumoto, H. Inoue, K. Yanaga, and M. Mori. 2007. Clinicopathological and biological significance of mitotic centromere-associated kinesin overexpression in human gastric cancer. *Br. J. Cancer* **97**:543–549.
 26. Ogawa, T., R. Nitta, Y. Okada, and N. Hirokawa. 2004. A common mechanism for microtubule destabilizers—M type kinesins stabilize curling of the protofilament using the class-specific neck and loops. *Cell* **116**:591–602.
 27. Ohi, R., M. L. Coughlin, W. S. Lane, and T. J. Mitchison. 2003. An inner centromere protein that stimulates the microtubule depolymerizing activity of a KinI kinesin. *Dev. Cell* **5**:309–321.
 28. Ohi, R., T. Sapra, J. Howard, and T. J. Mitchison. 2004. Differentiation of cytoplasmic and meiotic spindle assembly MCAK functions by Aurora B-dependent phosphorylation. *Mol. Biol. Cell* **15**:2895–2906.
 29. Parra, M. T., R. Gomez, A. Viera, J. Page, A. Calvente, L. Wordeman, J. S. Rufas, and J. A. Suja. 2006. A perikinetochoric ring defined by MCAK and Aurora-B as a novel centromere domain. *PLoS Genet.* **2**:e84.
 30. Segerman, B., P. Holmfeldt, J. Morabito, L. Cassimeris, and M. Gullberg. 2003. Autonomous and phosphorylation-responsive microtubule-regulating activities of the N-terminus of Op18/stathmin. *J. Cell Sci.* **116**:197–205.
 31. Sellin, M. E., P. Holmfeldt, S. Stenmark, and M. Gullberg. 2008. Global regulation of the interphase microtubule system by abundantly expressed Op18/stathmin. *Mol. Biol. Cell* **19**:2897–2906.
 32. Shimo, A., C. Tanikawa, T. Nishidate, M. L. Lin, K. Matsuda, J. H. Park, T. Ueki, T. Ohta, K. Hirata, M. Fukuda, Y. Nakamura, and T. Katagiri. 2008. Involvement of kinesin family member 2C/mitotic centromere-associated kinesin overexpression in mammary carcinogenesis. *Cancer Sci.* **99**:62–70.
 33. Stout, J. R., R. S. Rizk, S. L. Kline, and C. E. Walczak. 2006. Deciphering protein function during mitosis in PtK cells using RNAi. *BMC Cell Biol.* **7**:26.
 34. Vassilev, L. T., C. Tovar, S. Chen, D. Knezevic, X. Zhao, H. Sun, D. C. Heimbrock, and L. Chen. 2006. Selective small-molecule inhibitor reveals critical mitotic functions of human CDK1. *Proc. Natl. Acad. Sci. U. S. A.* **103**:10660–10665.
 35. Walczak, C. E., E. C. Gan, A. Desai, T. J. Mitchison, and S. L. Kline-Smith. 2002. The microtubule-destabilizing kinesin XKCM1 is required for chromosome positioning during spindle assembly. *Curr. Biol.* **12**:1885–1889.
 36. Walczak, C. E., T. J. Mitchison, and A. Desai. 1996. XKCM1: a *Xenopus* kinesin-related protein that regulates microtubule dynamics during mitotic spindle assembly. *Cell* **84**:37–47.
 37. Wordeman, L. 2005. Microtubule-depolymerizing kinesins. *Curr. Opin. Cell Biol.* **17**:82–88.
 38. Wordeman, L., and T. J. Mitchison. 1995. Identification and partial characterization of mitotic centromere-associated kinesin, a kinesin-related protein that associates with centromeres during mitosis. *J. Cell Biol.* **128**:95–104.
 39. Yuan, J., F. Eckerdt, J. Bereiter-Hahn, E. Kurunci-Csacsko, M. Kaufmann, and K. Strebhardt. 2002. Cooperative phosphorylation including the activity of polo-like kinase 1 regulates the subcellular localization of cyclin B1. *Oncogene* **21**:8282–8292.
 40. Yuan, J., A. Kramer, Y. Matthes, R. Yan, B. Spankuch, R. Gatje, R. Knecht, M. Kaufmann, and K. Strebhardt. 2006. Stable gene silencing of cyclin B1 in tumor cells increases susceptibility to taxol and leads to growth arrest in vivo. *Oncogene* **25**:1753–1762.
 41. Yuan, J., R. Yan, A. Kramer, F. Eckerdt, M. Roller, M. Kaufmann, and K. Strebhardt. 2004. Cyclin B1 depletion inhibits proliferation and induces apoptosis in human tumor cells. *Oncogene* **23**:5843–5852.
 42. Zhang, X., S. C. Ems-McClung, and C. E. Walczak. 2008. Aurora A phosphorylates MCAK to control ran-dependent spindle bipolarity. *Mol. Biol. Cell* **19**:2752–2765.
 43. Zhang, X., W. Lan, S. C. Ems-McClung, P. T. Stukenberg, and C. E. Walczak. 2007. Aurora B phosphorylates multiple sites on mitotic centromere-associated kinesin to spatially and temporally regulate its function. *Mol. Biol. Cell* **18**:3264–3276.
 44. Zhu, C., J. Zhao, M. Bibikova, J. D. Levenson, E. Bossy-Wetzel, J. B. Fan, R. T. Abraham, and W. Jiang. 2005. Functional analysis of human microtubule-based motor proteins, the kinesins and dyneins, in mitosis/cytokinesis using RNA interference. *Mol. Biol. Cell* **16**:3187–3199.